Digest Journal of Nanomaterials and Biostructures Vol. 6, No 3, July-September 2011, p. 1091-1101

NON-TOXIC NANOCOMPOSITE CONTAINING CAPTOPRIL INTERCALATED INTO GREEN INORGANIC CARRIER

I. F. ALEXA, R. F. POPOVICI[a], M. IGNAT, E. POPOVICI[*], V. A.VOICU [a]
Department of Materials Chemistry, Faculty of Chemistry, "Al. I.Cuza" University of Iasi, Romania
[a]University of Medicine and Pharmacy"Carol Davila", Department of Clinical Pharmacology and Toxicology, Bucharest, Romania

The purpose of this study is to investigate the influence of Mg/Al ratio of LDHs – as green inorganic carriers - on the potential ability to intercalate captopril - an angiotensin converting enzyme inhibitor-, and to release it in a controlled manner. LDHs matrices were exploited for the preparation of the controlled release formulations of captopril. The LDH-captopril nanocomposites have been synthesized through ion exchange treatment. With a view to making correlations between the loading capacity and release profiles of a loaded drug, the composites were characterized by XRD, N_2 sorption, FTIR, DSC-TG, particle size measurements and SEM were used. In order to determine the toxicity of the composites, the Kärber method was used. It was found that the loading capacity of captopril was directly correlated to the Mg/Al molar ratio of the matrices. LDH-captopril toxicity was lower than that of the pure captopril. The prepared delivery system has the advantage of a slow and gradual release pattern of the loaded drug, over a period of more than 30 h, opening the opportunity for the prospective use as potential controlled release formulation with only one daily administration.

(Received April 19, 2011; Accepted July 4, 2011)

Keywords: Layered double hydroxides, Captopril, release, ACE inhibitor, Nanocomposite, *G*reen carrier

1. Introduction

Layered double hydroxides (LDHs) are a class of ionic lamellar solids with positively charged brucite layers with two kinds of metallic cations and exchangeable hydrated gallery anions [1-5]. The general formula of LDHs can be represented by $[M^{II}_{1-x}M^{III}_{x}(OH)_2]^{x+}\ A^{n-}_{x/n}\ mH_2O$, where M^{II} and M^{III} are the divalent and trivalent cations that occupy the octahedral positions in the brucite-like sheets, A is the interlayer anion and $\boldsymbol{x}$ is the molar $M^{III}/M^{II}+M^{III}$ ratio [6].

It was shown that layered double hydroxides are one type of important green carriers which can accommodate beneficial polar organic compounds between their layers such as aminoacids [7], DNA [8], plant growth regulators [9], pesticide [10], and drugs [11,12].

Particularly, a lot of attention was paid on the organic–inorganic layered double hydroxides hybrid – containing biomolecules because of its unique properties, such as enhanced dissolution property, increased thermal stability and controlled release rate [13].

The interlayer anionic groups of pristine LDHs can be replaced by pharmaceutically active compounds. In this case, the pharmaceutically active compound is required to have at least one anionic group in order to be intercalated among the layers of LDHs [14]. Intercalation is defined as insertion of an organic guest into a preformed inorganic host leading to the host-guest supramolecular organic-inorganic hybrids [15].

Because the release of drugs from loaded LDHs are potentially controllable, these materials are the promising matrices in the pharmaceutical field for encapsulating functional biomolecules, drugs and other pharmaceutically active compounds [16].

[*]Corresponding author: eveline@uaic.ro; evelinepopovici@yahoo.com

There are many papers which describe the loading of drugs or biomolecules into the brucite layers, the release behaviors of drugs under different physiological conditions [17], and the toxicity tests of LDHs to the cells or *in vivo*. These experiments underlined the advantages of LDHs-carriers: as good biocompatibility, low toxicity, capacity of a full protection for the loaded drugs among the interlayers [18,19].

LDHs are able to upload and retain drugs by intercalating them among layers and to release them in a desired controlled way.

The drug selected for intercation in this system was captopril. As well known, captopril is an angiotensin-converting enzyme inhibitor commonly used for the treatment of arterial hypertension. The dimensions of captopril molecule are of 0.9 x 0.57 x 0.33 nm. Captopril was previously used as incorporating drug in various other delivery systems [12].

The purpose of this study is to investigate the impact and degree of influence of the Mg/Al molar ratio of brucite layers on the capability to load captopril and release it in a controlled manner.The study also investigated the toxicity of LDH and LDH captopril system.

2. Experimental

2.1. Materials

All nitrates $Mg(NO_3)_2 \cdot 6H_2O$, $Al(NO_3)_3 \cdot 9H_2O$ used in the experiment were purchased from Aldrich Chemicals. Commercial captopril tablets of 25 mg from S.C.Terapia S.A. Cluj-Napoca were used, containing 25 mg captopril per tablet.

2.2. Synthesis of the nitrate forms of Mg_x-Al-layered double hydroxides

The nitrate forms of Mg_xAl-layered double hydroxides with the Mg:Al ratios of 3:1, 2:1 and 1:1, were synthesized by co-precipitation method, at a constant value of pH=8.

In a typical synthesis, to a desired mixed metal nitrates solution (1M in total), at room temperature, and under N_2 atmosphere to avoid, or at least minimize the contamination with atmospheric CO_2, under magnetic stirring, was added 2M NaOH solution until the pH reached value 8 and remained constant at that level [20]. After precipitation, the slurry was kept for 3 hours at room temperature, followed by ageing at 343K for 24 hours.

The resulted solid was separated by filtration, washed several times with de-ionized water and dried at 353K over night.

The obtained products were noted Mg_xAl-LDH, where *x* stands for the Mg/Al molar ratio in initial mixture.

2.3. Intercalation of captopril into LDHs

In order to prepare the desired drug delivery system, the obtained Mg_xAl-layered double hydroxides were used as host matrices for storage of captopril loaded by ion exchange process. The loaded quantity of captopril, reflecting the loading capacity of the system, was evaluated as function of chemical composition of matrices, expressed by Mg/Al molar ratios.

Before impregnation process, one gram of the LDH powder was dried at 200^{o}C for 2 hours, and then the material was impregnated with 100 mL of captopril aqueous solution (50 mg/L) and stirred vigorously at room temperature for 3 days under N_2 atmosphere [7]. The resulting mixture was filtered, dried and used for subsequent investigations.

2.4. Characterization

X-ray diffraction analysis (XRD) was employed to identify and characterize the morphology of the synthesized materials. The XRD patterns were recorded using a TUR M-62 powder diffractometer system with CuKα radiation (K_α = 0.1518 A°, 36 kV, 20 mA), a voltage of 36 kV, a current of 20 mA, and a goniometer speed of 0.5°/min). The samples were scanned for 2θ values ranging from 5 to 70°.

The infrared spectra were performed on a SPECORD Carl Zeiss Jena FT-IR spectrometer (KBr pellets). Porosity and surface area were obtained from the N_2-sorption isotherms performed on a NOVA 2200e system using nitrogen as the adsorbate at liquid nitrogen temperature (-196 °C). All the samples were outgassed under vacuum, for 6 hours at 298K before adsorption measurements. The surface area was calculated using the BET method in the range of relative pressure 0.05-0.35. Pore volume was calculated at the relative pressure of 0.95. Pore sizes distributions were calculated from the adsorption branches of the N_2 adsorption isotherms using the Barett -Joyner-Halenda (BJH model).

The thermal behavior data were obtained on STA 429 system using range 20°C/20.0(K/min)/800°C for sample DSG(/TG) HING RG 3/S.

Particles size distribution and mean pore diameter (D_p, nm) measurements were recorded using an optic measurement device SALD-7001 type Laser Diffraction Particle Size Analyzer (Shimadzu, Japan).

The SEM images were obtained using a JSM 5510 microscope, operating at an accelerating voltage of 15 kV.

2.5. In vitro drug release

A simulated intestinal environment was created using a phosphate-buffered saline media (PBS).

PBS is a buffer solution commonly used in biological research. It is a water-based salt solution containing sodium chloride 137 mmol/L, sodium phosphate 8.1 mmol/L, and (in some formulations) potassium chloride 2.7 mmol/L, and potassium phosphate 1.76 mmol/L.

In PBS solution, the *in vitro* drug release was tested at pH of 7.4, with a solid/liquid ratio of 0.1g/100mL at 37 ± 2 ºC for a period of 30 hours. A sample of 10 mL was withdrawn at predetermined intervals and centrifuged. The amount of released captopril, accumulated in the PBS solution was measured using UV-Vis spectrophotometer at fixed wavelength of 257.5 nm.

3. Results and discussion

3.1. Loading capacity variation with Mg/Al molar ratio

The variation of the loading capacity with the Mg/Al molar ratio is presented in Table 1.

Table 1. The influence of Mg/Al molar ratio on loading capacity

Sample	Mg/Al ratio	Loading capacity, % wt captopril
LDH-MgAl	$[Mg_{0.63}Al_{0.63}(OH)_2]$	11.3%
LDH-Mg_2Al	$[Mg_{0.63}Al_{0.32}(OH)_2]$	17.5%
LDH-Mg_3Al	$[Mg_{0.63}Al_{0.21}(OH)_2]$	22.7%

The powder of Mg_xAl-NO_3 matrices were chosen for captopril loading process, based on ion-exchange, at room temperature. The above representation denotes a strong dependence between the captopril amount loaded and the chemical parameter of matrix, expressed by Mg/Al molar ratio. Due to the fact that Mg_3Al-LDH loaded the highest quantity of captopril compared to the captopril concentration of the usual oral commercial formulation (21 wt %), in the following tests we chose to use this matrix.

3.2 Dimensional matrix characterization

The pristine Mg_3Al-LDH matrix is a white powder, having a particle size distribution presented in (Fig.1), as an average of the three consecutive measurements. The particle size volumetric distribution of Mg_3Al-LDH appeared to be bimodal, with particles averaging about 0.7 μm. Representing the numerical histogram we could say that the particle size distribution is unimodal with the particle diameter of 0.3 μm. Measured values of the particle size distribution in LDH are detailed in Table 2.

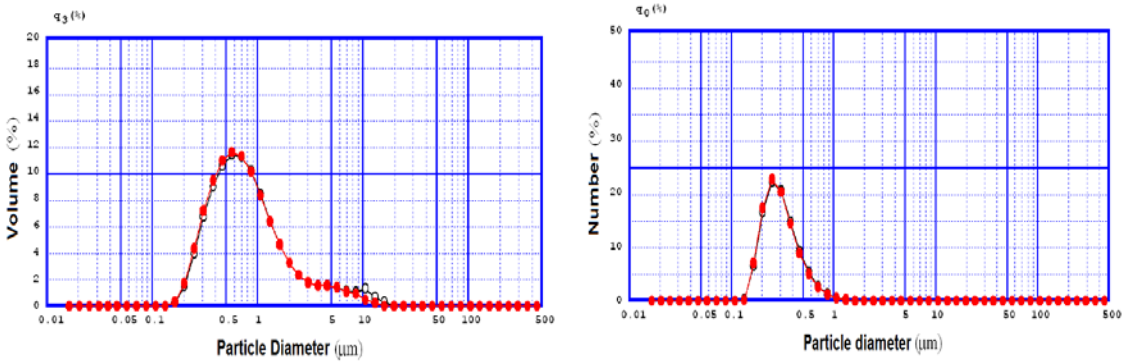

Fig.1. Numerical and volumetric histogram of the particle size distribution for Mg_3Al-LDH matrix.

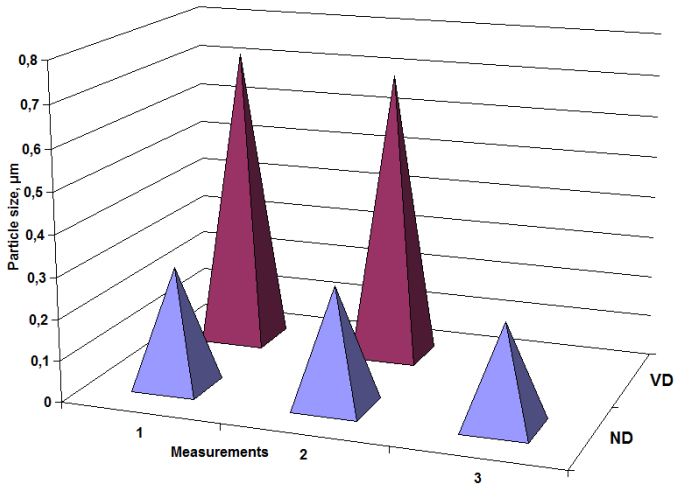

ND-Numerical Distribution; **VD**- Volumetric Distribution

Fig. 2. Measured values of the particle size distribution in LDHs

3.3. XRD results

The matrices show diffraction patterns which are typical for the double layer hydroxides structure with sharp and symmetric reflections of the basal (003), (006) planes and broad, less intense asymmetric reflections for nonbasal (101) and (015) planes. The pick from 2θ= 61.6° is due to (110) plane [19].

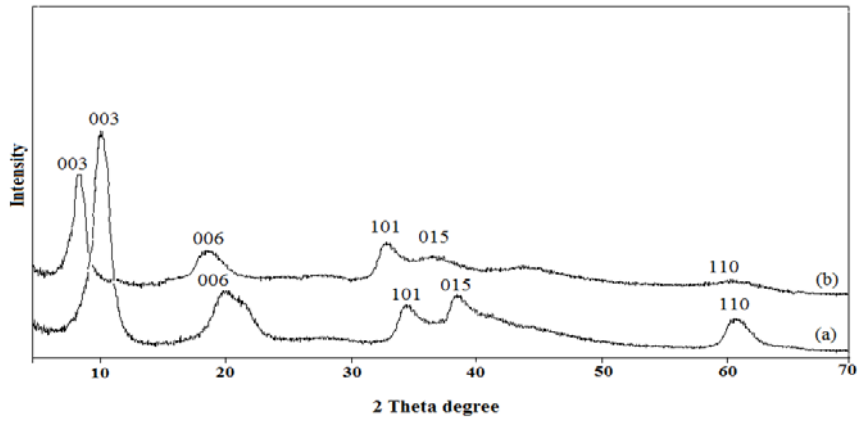

Fig. 2. Powder XRD patterns of (a) Mg_3Al-LDH matrix and (b) intercalated captopril sample Mg_3Al-LDH - captopril

The calculated basal spacing and lattice parameters (Table 1) are in agreement with the values reported in the literature indicating the formation of well-crystallized small LDH nanoparticles having nitrate anions in the interlayer gallery [21].

The **a** parameter of LDH, corresponding to the cation-cation distance within the brucite-like layer, can be calculated with the following formula $\mathbf{a} = 2 \times 2d_{110}$. The **c** parameter is related to the thickness of the brucite-like layer and the interlayer distance and can be deducted from the formula $\mathbf{c} = 3d_{003}$. The results are shown in Table 3.

Table 3. Structural characteristics of the synthesized LDH samples

Sample	d_{003}, Å	*c*, Å	d_{110}	*a*, Å
Mg_1Al-LDH	7.60	22.80	1.49	2.98
Mg_2Al-LDH	8.02	24.06	1.50	3.00
Mg_3Al-LDH	8.41	25.23	1.51	3.02
Mg_3Al-LDH -Captopril	14.60	43.80	1.51	3.02

The literature data have indicated that the basal **d** spacing of the (003) plane is dependent on the size of the guest anion in the interlayer of the NO_3^- form of LDH.

In Fig.2., the X-ray diffraction patterns of NO_3^- form of LDH and captopril–LDH system were compared, and the basal **d** spacing value of NO_3^- -LDH layer was 8.75Å (2θ=10.10°); however, the basal reflection (003) of captopril - LDH shifts to lower 2θ (for 003 reflection: 2θ=7.48°) that is expanded to 14.60Å, indicating the intercalation of captopril into the interlayer of Mg–Al-LDH.

The interlayer distance $\mathbf{d}_{003}$ of 14.60 Å, representing the combined thickness of the brucite–like layer (3.02 Å) and the gallery height, is higher after captopril ion-exchange compared with pristine LDH (Fig. 2) suggesting a successful captopril intercalation.

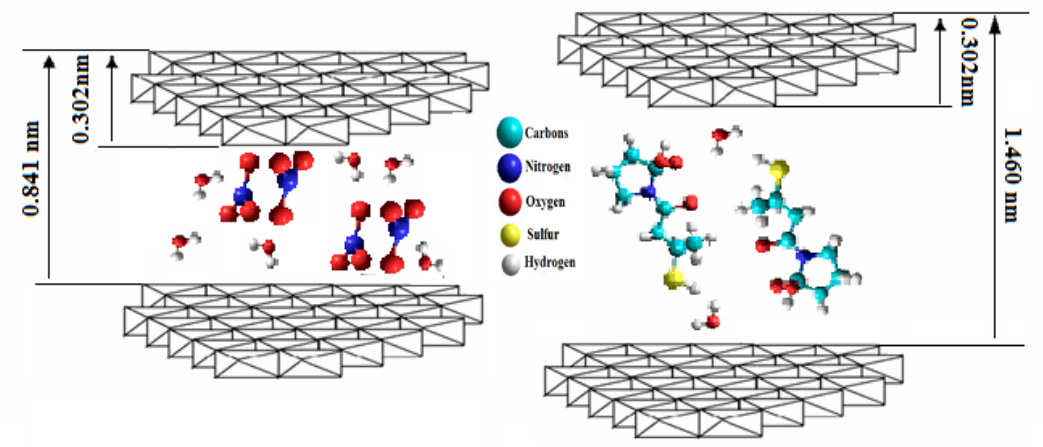

Fig. 3. Schematic structure representation of Mg_3Al-NO_3 - LDH and Mg_3Al-LDH –captopril samples

3.4 FT-IR spectra

The intercalation mode of captopril into prepared matrices can be proved easily by FTIR analysis, comparing the spectrum of the host matrix with that intercalated with captopril, as depicted in Figure 4.

The broad absorption bands at 3446 - 3449 cm^{-1}, respectively, arise from the stretching modes of hydroxyl group in the brucite-like layers and interlayer water molecules (Fig.4b and 4c), with occur at lower frequency in the region of 3400-3600 cm^{-1} due to the formation of hydrogen

bonds between interlayer water and guest anions as well as the hydroxide groups of the host layers [22].

The FTIR spectrum of captopril shows the presence of the weak peaks, centered at 2880 cm^{-1}, 2940 cm^{-1} and 2980 cm^{-1} that could be attributed to the asymmetric C-H stretching vibration of captopril anions (Fig.4a) and also the characteristic bands at 1749 cm^{-1}, due to υ_{as} (COOH) and the band at cm^{-1}, attributed to υ (S-H).

At the same time, the strong absorptions at 1592 and 1365 cm^{-1}, are indicative of the υ_{as} (COO^-) and υ_s (COO^-), respectively, of the -COO^- groups in pure captopril in line with dissociation properties of these two groups [16]. Also, the band at 1445 cm^{-1}, is due to the quaternary C atom and the one at 1205 cm^{-1} to the υ (C-N) in captopril molecule. The band at 657 cm^{-1} is assigned to the M-O lattice mode [23].

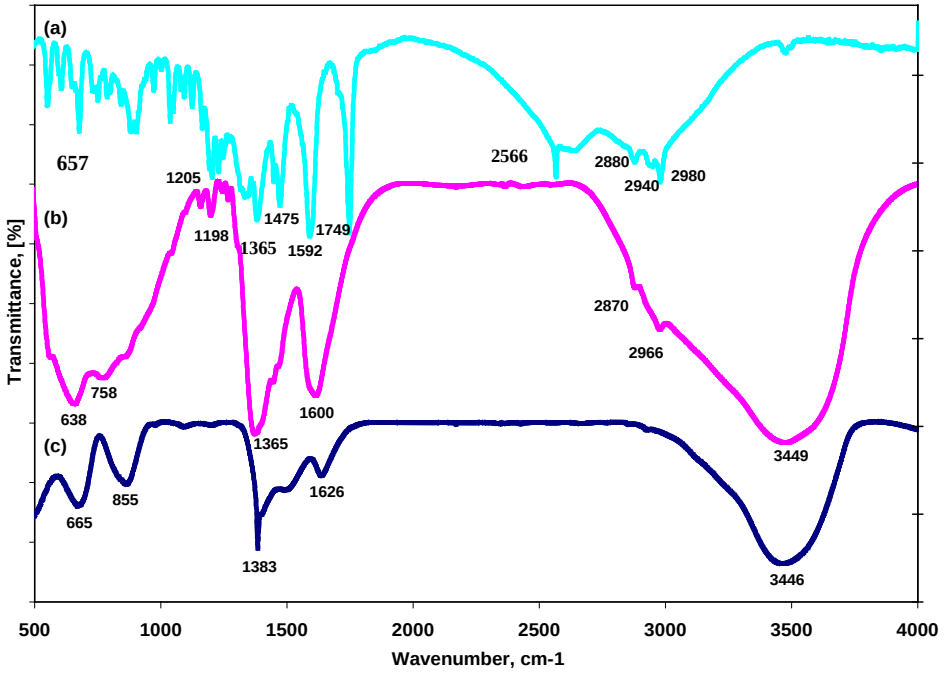

Fig. 4. FTIR spectra of (a) Captopril, (b) Mg_3Al-LDH -captopril, (c) Mg_3Al-LDH

Upon intercalation of captopril, the red shift in the stretching frequency of carboxylate anion of captopril provides evidence that the drug is electrostatically bonded to LDHs, as previously reported by H. S. Panda [24].

3.5 Nitrogen adsorption/desorption isotherms

The N_2-sorption measurements were used to characterize the textural properties of the synthesized materials. As result, were obtained the isotherms and the corresponding pore size distributions, as shown in the Fig.5.

According to IUPAC classification [25], all isotherms are of type IV, characteristic for mesoporous materials, showing a hysteresis loop. In both cases, the hysteresis loops are identifiable as H_3 type that usually is given by the aggregates of platy particles or adsorbents containing slit-shaped pores. Their different appearances suggest differences in porosity characteristics after captopril intercalation.

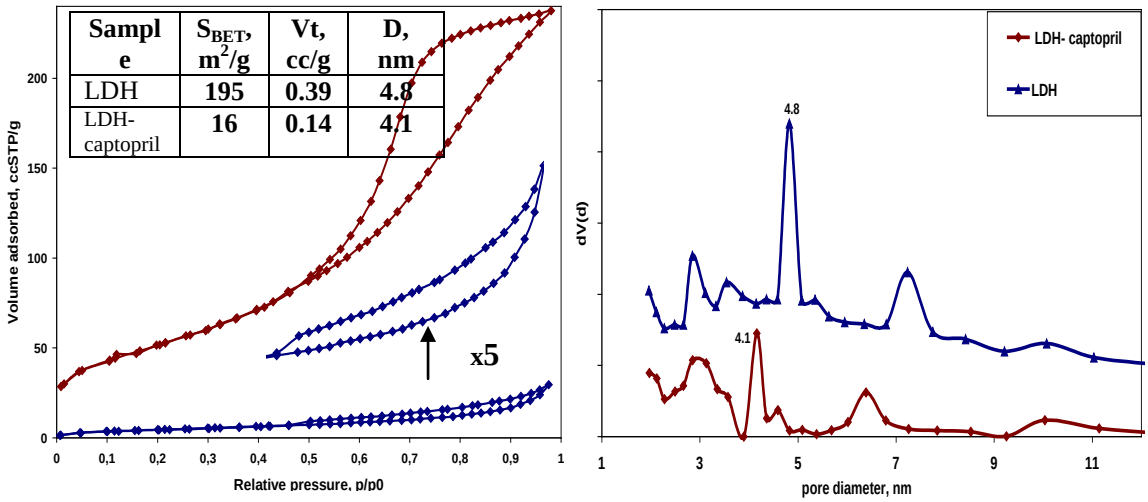

Fig. 5. The N_2 adsorption/desorption isotherms and pore size distributions.

The broadness of the hysteresis loop leads to a large pore size distributions. Looking at the pore size distributions of the samples we noticed that the structures contain voids having a highly non-uniform sizes and/or shapes.

The BET specific surface areas, pore sizes, and the total pore volumes decrease after the drug loading, confirming the intercalation of the drug between brucite layers of LDH.

3.6 Thermal analysis

The TG and DSC idem profiles of the studied samples are illustrated in Fig. 6. For pure captopril powder (Fig.6a), the DSC curve shows three main thermal events. The first thermal event occurs in the region of 90-190 °C, which corresponds to a sharp endothermic peak centered at 98 °C in the DSC curve, is attributed to the captopril melting and it is also associated to water removal. The second thermal event occurs in the region of 200-350 °C, which corresponds to the endothermic peak centered at 258 °C, is due to the thermal decomposition of captopril, in good correlation with literature data [26] The last event, which occurs in the 370-600 °C temperature range, is due to the burning out of captopril and is represented by a sharp exothermic peak centered at 407 °C.

The LDH-captopril nanocomposite shows the TG and DSC curves presented in Fig.6b. It could be observed four stages of weight losses. The processes which occur in the temperature range of 50-160 °C, are assigned to the losses of both captopril melting and interlayer water. The next weight loss occurs in the range 180-300°C and corresponds to the dehydroxylation of the brucite layers and also to the captopril combustion from the edges or from the surface of the crystallites, represented by an exothermic peak in the DSC diagram. The last mass loss occurs between 300-540°C and is the result of the complete decomposition of the intercalated captopril and characterizes by a sharp exothermic peak in DSC curve. The total amount of loaded captopril was calculated to be of 22.7 wt % that is in good agreement with the maximum o loading capacity. Also, it is observed that the thermal stability of captopril is potentiated after intercalation into brucite layers.

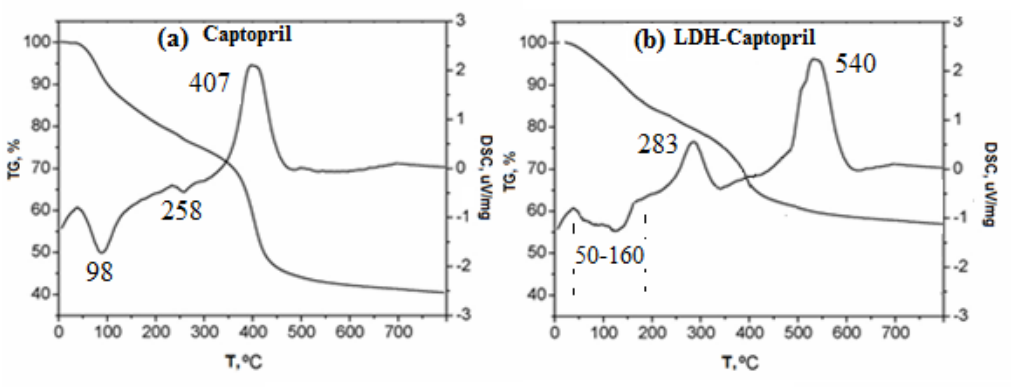

Fig. 6. DSC- TG profiles of Captopril (a), Mg_3Al-LDH –Captopril (b)

3.7 SEM micrograph

From the Fig. 7 it can be observed that the spherical particles of captopril are attached to the LDHs surface. Compared with non-intercalated LDHs material, $CapH_2$-intercalated LDHs form agglomerations, which appear due to the modification of LDHs surface by organic compound intercalation.

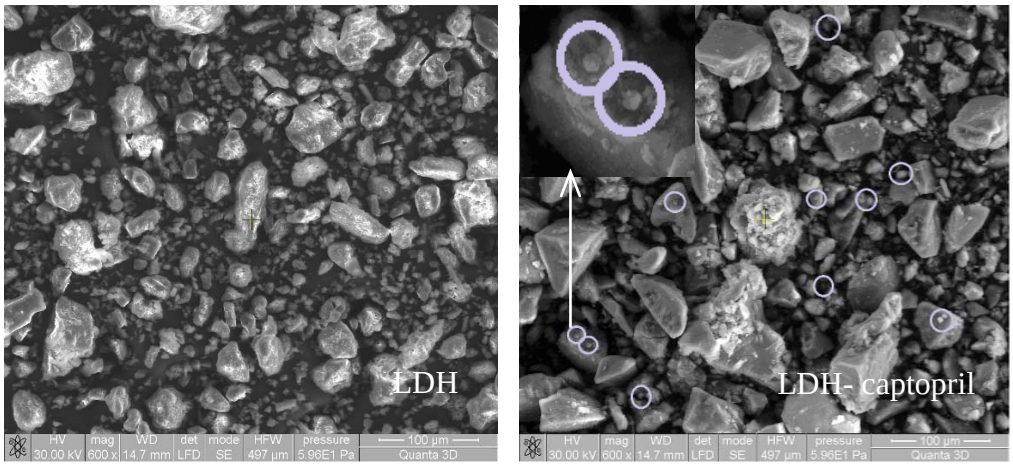

Fig.7. SEM micrograph of the Mg_3Al-LDH and LDH –captopril

3.8 Drug release

Knowing the basicity of LDHs, their use in drug delivery systems is questionable for the gastric environment, where the pH is of 1-2, and determines the partial dissolution of brucite layers.

In vitro release properties of the LDH-captopril system were investigated in simulated intestinal fluid, pH=7.4**,** using phosphate buffer solution. The comparison between oral commercial captopril formulation, grounded with sub-micron particles, and Mg_3Al-LDH-captopril powder nanocomposites was studied (Fig.8).

We observed that even after 30 hours of observation, a certain amount of captopril still existed in the synthesized systems. The amount of released captopril, after 4 hours of observation, represented 28.7 wt. % for LDH-captopril and 57.9 wt. % for the commercial formulation of captopril.

The Mg_3Al-LDH-captopril powder has the advantage of the gradual release over a longer time period as demonstrated by the presence of captopril in the solid formulation, even after 30 hours of observation.

In order to analyze the data obtained from the *in vitro* release studies and to evaluate the kinetic release mechanism, we used the Korsmeyer and Peppas equation - a simple, semi-empiric model, when diffusion is the main drug release mechanism, relating exponentially the drug release to the elapsed time (t):

$$F = k^{tn}$$

In which K is a kinetic constant characterizing the drug–carrier system, while n is an exponent that characterizes the mechanism of drug release. If the exponent $n \leq 0.45$, then the drug release mechanism is a Fickian diffusion and if $0.45 < n < 0.89$, then it is a non- Fickian or anomalous diffusion.

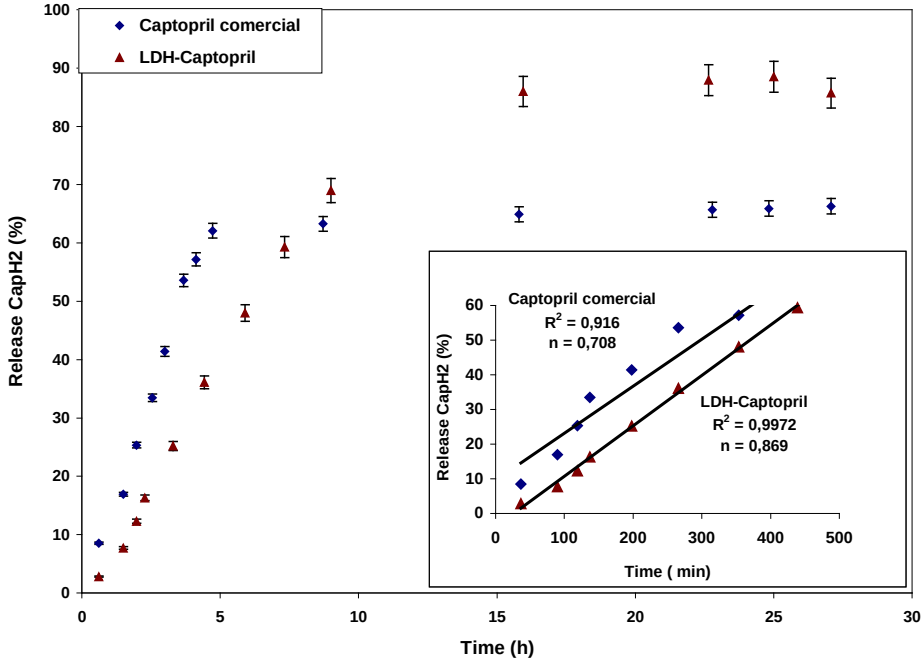

Fig.8. Captopril release in simulated intestinal fluid (PBS) and the representation of "n" pattern calculated from the Korsmeyer–Peppas.

The initial 60% of captopril release at pH 7.4 fitted with the Korsmeyer–Peppas model (Fig.8 bottom right), exponent "*n*" revealed that the captopril release mechanism from the commercial formulation was more diffusion-based (n = 0.708) than in the case of LDH-captopril sample (n = 0.869) [13, 14]. Therefore, the obtained results calculated according to the Korsmeyer–Peppas model, show that the samples obtained by loading the drug in LDHs show the non-Fickian diffusion mechanism. It can be see a good linearity between captopril releases in time: the regression coefficient R^2 ranging from 0.9160 to 0.9972.

3.9 Toxicity Analysis

A dose response on the toxicity was studied using by Trimmed Spearman Karber method in Sprague-Dawley rats, after oral administration of the samples in animals.

According to the Hodge and Sterner toxicity scale, the substances with LD_{50} between 5'000 – 15'000 mg/kg display a very low toxicity, being practically non-toxic [15]. While the LD_{50} for captopril was evaluated at about 6590 mg/kgc, the toxicity values of the synthesized materials were 7410 mg/kgc and 7315 mg/kgc for LDH and LDH-captopril, respectively. Evaluated by the Trimmed Spearman Karber method, combinatia LDH-captopril proved to be non-toxic for human beings (Fig.9).

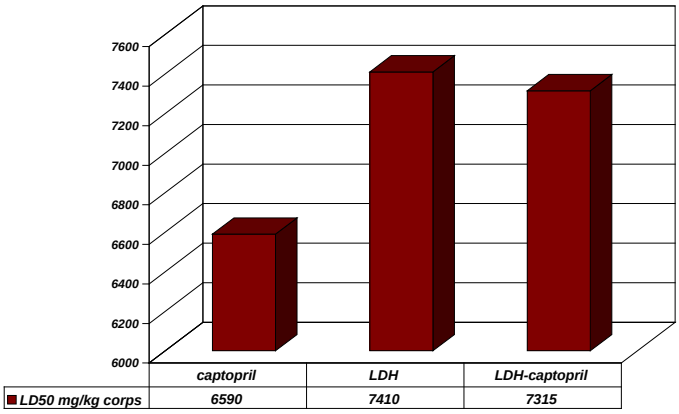

Fig.9. The Hodge and Sterner Toxicity Analysis.

4. Conclusions

Mg_xAl-LDH matrices- green carriers, having Mg/Al molar ratio of 1/1 to 3/1, and average particle size of 274 nm, synthesized by coprecipitation method were subjected for the study of their potential ability to intercalate an antihypertensive agent, as captopril - an angiotensin-converting enzyme inhibitor-, in order to storage, transport and release it in a controlled manner. The LDH-captopril nanocomposites with intercalated antihypertensive agent were synthesized through ion exchange treatment.

It was found that the loading capacity of captopril was directly correlated to the Mg/Al molar ratio of matrices and the toxicity of intercalated captopril is lower than the pure captopril. The advantages of the prepared delivery systems are the gradual captopril release behavior over a period of more than 30 h, and the lack of toxicity, which opens the opportunity for their prospective uses as for considering it as potential formulation with only one daily administration.

Acknoledgments

This study was supported by POSDRU/88/1.5/S/47646 project, funded by European Social Fund, POSDRU 2007-2013.

References

[1] Braterman, P. S.; Xu, Z. P.; Yarberry, F. Chemistry of layered double hydroxides. In Handbook of Layered Materials; Auerbach, S. A., Carrado, K. A., Dutta, P. K., Eds.; Marcel Dekker: New York, p. 373, (2004).
[2] Rives, V. Layered Double Hydroxides: Present and Future; Nova Science Publishers: New York, NY, USA, (2001).
[3] Williams, G.R.; O'Hare, D. Towards understanding, control and application of layered double hydroxide chemistry. J. Mater. Chem., **16**, 3065-3074, (2006).
[4] Khan, A.I.; O'Hare, D. Intercalation chemistry of layered double hydroxides: Recent developments and applications. J. Mater. Chem. **12**, 3191-3198, (2002).
[5] Guo, X.; Zhang, F.; Evans, D.G.; Duan, X. Layered double hydroxide films: Synthesis, properties and applications. Chem. Commun. **46**, 5197-5210, (2010).
[6] S. M. Auerbache, K. A. Corrado, P. K. Dutta, Handbook of layered materials, pp. 373-449, (2004).
[7] Kwak, S.-Y.; Kriven, W. M.; Wallig, M. A.; Choy, J.-H. Biomaterials **25**, 5995, (2004).

[8]Ladewig, K.; Niebert, M.; Xu, Z.P.; Gray, P.P.; Lu, G.Q.M. Efficient RNA delivery to mammalian cells using layered double hydroxide nanoparticles. Biomaterials **31**, 1821-1829, (2010).
[9] Z.Hussein, Z. Zainal, A. H. Yahaya and D. W. Foo, Journal of Controlled Release **82**(2-3), 417-427 (2002).
[10] I. Pavlovic, C. Barriga, M.C. Hermosín, J. Cornejo and M.A. Ulibarri, Clay Minerals, **43**(2), 155 (2008).
[11] Yan Yuan, Wenfang Shi, Progress in Organic Coatings 69, pp. 92–99 , (2010).
[12] R. F. Popovici, E. M. Seftel, G. D. Mihai, E. Popovici, V. A. Voicu, Journal of Pharmaceutical Sciences, **100**(2), 704 (2011).
[13] Ye Kuang, Lina Zhao, Shuai Zhang, Fazhi Zhang, Mingdong Dong, Sailong Xu**,** Materials, **3**, 5220 (2010).
[14] Wei, M.; Pu, M.; Guo, J.; Han, J.; Li, F.; He, J.; Evans, D.G.; Duan, X. Intercalation of L-dopa into layered double hydroxides: Enhancement of both chemical and stereochemical stabilities of a drug through host-guest interactions. Chem. Mater. **20**, 5169-5180, (2008).
[15] Wei, M.; Yuan, Q.; Evans, D.G.; Wang, Z.; Duan, X. Layered solids as a 'Molecular Container' for pharmaceutical agents: L-tyrosine-intercalated layered double hydroxides. J. Mater. Chem. **15**, 1197-1203 (2005).
[16] H.Zhang, S.H.Guo, K.Zou, X.Duan, Mat.Research Bulletin, **44**, 1062-10699, (2000).
[17] Wei, M.; Pu, M.; J. Guo, Han, J.; Li, F.; He, J.; Evans, D.G.; Duan, X. Intercalation of L-dopa into layered double hydroxides: Enhancement of both chemical and stereochemical stabilities of a drug through host-guest interactions. Chem. Mater. **20**, 5169 -5180, (2008).
[18] S.-J. Choi, J.-M. Oh, J.-H. Choy, Human-related application and nanotoxicology of inorganic particles: Complementary aspects. J. Mater. Chem. **18**, 615, (2008).
[19] E. M. Seftel, E. Popovici, E. Beyers, M. Mertens, H. Y. Zhu, P. Cool, E. F. Vansant, New MgAl-LDH/TiO_2 nanocomposites with photocatalytic application , J.Nanoscience Nanotechnol. **10** (12), pp. 8227-8233, (2010).
[20] M. Wei, S.X. Shi, J. Wang, Y. Li and X. Duan, J. Solid State Chem. **177,** 2534–2541, (2004).
[21] J. Olanrewaju, B. L. Newalkar, C. Mancino, S. Komarneni, Materials Letters **45**, 307 (2000).
[22] K. Nakamoto, Infrared and Raman Spectra of inorganic and Coordination Compounds, 5.th Edition, Wilez, New York, (1997)
[23] F.Y. Qu, G.S. Zhu, S.Y. Huang, S.G. Li, J.Y. Sun, D.L. Zhang and S.L. Qiu, Micropor.Mesopor. Mater. **92**, pp. 1–9, (2006).
[24] H. S. Panda, R. Srivastava, D. Bahadur**,** J. Phys. Chem. B, **113** (45), 15090 (2009).
[25] Jean Rouquerol, Françoise Rouquerol, Kenneth Sing, Adsorption by powders and porous solids, ISBN 10: 0-12-598920-2, (1998).
[26] R. Gupta, C.N.Shanthi, Arun K Mahato, International Journal of Drug Development & Research, **2**, Issue 2, (2010).
[27] F.Li, X. Duan, Struct.Bond **119**, 193 (2006).
[28] M. Del Arco, S. Gutie′rrez, C. Martı′n, V. Rives and J. Rocha, J. Solid State Chem. **177,** 3954 (2004).